

# Entropy production minimization as design principle for membrane systems: Comparing equipartition results to numerical optima

Elisa Magnanelli,<sup>\*</sup> Eivind Johannessen, and Signe Kjelstrup

*Department of Chemistry, NTNU - Norwegian University of Science and Technology,  
N-7491 Trondheim, Norway*

E-mail: elisa.magnanelli@ntnu.no

## Abstract

Entropy production minimization procedures presented in literature show that, under different assumptions, the optimal solution might be characterized by different thermodynamic quantities being constant. These constant quantities might be the local entropy production, the thermodynamic driving forces, the thermodynamic speed, or the thermodynamic length. After presenting the assumptions made in the different derivations, we use the results as design principles to reduce entropy production in a membrane unit for CO<sub>2</sub> separation from natural gas, and we compare them to the numerically determined optimum.

For a continuous process, we consider the equipartition of forces (EoF), the equipartition of entropy production (EoEP), and the equal thermodynamic speed (ETS) results. When we can independently control all driving forces, the numerical optimum and EoEP coincide. Even though EoF and ETS differ from the optimum, they approximate it well. When the transport coefficients are constant, EoF follows from EoEP. If the optimization was carried out with fixed number of relaxations instead of fixed

length of the membrane unit, the thermodynamic speed would then be constant in the optimal case. When the thermodynamic driving forces cannot be controlled independently, neither of the equipartition results characterizes the optimal solution. However, EoEP and ETS approximate it well. Since EoEP and ETS give good approximations of (or coincide with) the numerical optimum independently of the type of control, they can be used as design principles to reduce entropy production in membrane systems. However, using an equipartition result as a design principle will generally not give one and only one solution, and some equipartitioned designs may be far from the optimum. For a discrete process, we considered the EoEP and the equal thermodynamic length (ETL) results. In this case, EoEP gives the best approximation of the optimum. Since the process is not an equilibration process, ETL does not coincide with the optimum, but it still approximate it well.

## 1 Introduction

The worldwide increasing concerns about energy savings make thermodynamic optimization a relevant topic. The purpose of thermodynamic optimization is to minimize the losses of useful work in a process. Such losses were first related to the production of entropy by the Gouy-Stodola theorem,<sup>1</sup> which was then generalized by the work of Hoffmann et al<sup>2</sup> and Badescu.<sup>3</sup>

Many studies on entropy production minimization have been carried out over the years, and great efforts have been put into finding out what features characterize the most energy efficient processes.

Different results of entropy minimization procedures have been presented in the literature. Often, the features that characterize the results have been claimed to be general and proposed to be used as design principles. However, when the results depend on the assumptions that are made on the process or on the optimization, their translation to general design principles may not be straightforward. This paper will address under what conditions such results

correspond to the optimum and under which others they differ. We will also evaluate their performances as design principles for minimization of entropy production in a membrane system.

The use of equipartition of entropy production (EoEP) as design principle was first proposed by Tondeur and Kvaalen,<sup>4</sup> who observed that the best configuration for a process operation is the one where the local entropy production is uniformly distributed. This result was derived under conditions for which constant entropy production coincided with constant driving forces and fluxes. Equipartition of entropy production had already been observed by others in systems such as heat engines.<sup>5</sup>

Inspired by Tondeur and Kvaalen, Sauar et al.<sup>6</sup> proposed equipartition of forces (EoF) as design principle. They stated that two process streams exchanging fluxes need to have uniform driving forces over the transfer surface in order to minimize the entropy production. The theoretical principle was derived from irreversible thermodynamics and Cauchy-Lagrange optimization procedures. Even though the transport coefficients were allowed to vary as functions of the state variables, the transport path between the streams were considered to be independent. This last condition implies that the conservation equations that govern the process streams are not taken into account in the optimization procedure. Later, Bedeaux et al.<sup>7</sup> clarified that the freedom to change the process plays a fundamental role in the results of the optimization procedure, and that EoF applies only if the transport paths are independent and all kind of possible variations of the process streams are considered, even the unfeasible ones. They recognized that the iso-force solution could probably not be realizable in practice.

However, EoF has been applied to different constrained systems, such as heat exchangers,<sup>8,9</sup> distillation columns,<sup>10-12</sup> and chemical reactors.<sup>13-15</sup> Despite the fact that EoF does not strictly apply to the considered systems, the entropy production was strongly reduced by using EoF as a design criterion. This has been interpreted as a sign that the entropy production space has a rather flat minimum.<sup>12,16</sup>

In practice, systems are subject to governing equations that need to be taken into account. Johannessen et al.<sup>16</sup> gave the general solution of the entropy production minimization problem for a system obeying conservation equations. In the specific case, the systems was described by one control variable and, thus, one governing equation. The result was applied to a heat exchanger where the energy conservation equation described one of the sides. The only considered assumptions were those of linear flux-force relations and of transport coefficients dependent on the state variable only (i.e. the transport coefficient is not a direct function of the system coordinates). Thanks to these assumptions, the Lagrangian of the optimal problem was autonomous, and thus constant in space. Calculus of variations or optimal control theory can then be used to prove that the local entropy production needs to be constant in order for the total entropy production to be minimum. They also showed that EoEP implies EoF, when the system lacks memory of prehistory (i.e. the transport coefficients and the proportionality factor matrix of the optimal control theory formulation are constant<sup>17</sup>). When this condition does not apply, EoEP does not correspond to EoF.

The large number of optimization studies on heat exchangers<sup>8,9,18-20</sup> is due not only to the fact that heat exchangers have a very wide range of applications, but also that they are relatively simple systems that can be used to illustrate fundamental concepts. However, the fact that only heat transport takes place in such systems makes the thermodynamic driving force controllable by control of one of the streams' temperature only. For long, this fact may have hidden the implicit assumption that the control on the system needs to be sufficient to independently control *all* driving forces. Without this assumption, none of the equipartition results holds.<sup>17</sup> Nevertheless, EoEP as a design principle to minimize entropy production has been applied to systems where this condition did not hold, such as diabatic distillation.<sup>21</sup> Even though the result does not strictly apply in this case, it was found to give a good approximation of the mathematical optimum.

Finite-time thermodynamics was developed in the early seventies as a response to the world oil crisis.<sup>22</sup> The goal of the theory was to find bounds for thermodynamic processes

subject to time constraints, more realistic than the limit given by the reversible process. At first, the focus of the finite time analysis was directed to heat engines.<sup>23–25</sup> A fundamental concept was introduced to define a new bound for real processes, the thermodynamic length.<sup>26</sup> This was defined on the basis of the equilibrium thermodynamic metric proposed by Weinhold.<sup>27</sup> Salamon and Berry<sup>28</sup> found that the square of the thermodynamic length is related to the lower bound of a process dissipation, when the process is endoreversible and it is a quasi-static step process. The definition of endoreversible process was given by Rubin<sup>24</sup> as a process where the process streams undergo reversible transformations only, while all irreversibilities take place at the boundary with the ambient. A quasi-static step process is a process where the system is brought from a given initial state to a given final state along a series of equilibration steps. Under these assumptions, minimum dissipation gives equal thermodynamic length (ETL) between consecutive steps. Moreover, if the total time allocated to the process is much larger than the relaxation time of the system, the same number of relaxation times should be allocated to each equilibration step, in order to get the process optimum. Thus, the concept of thermodynamic speed was introduced, defined as the derivative of the thermodynamic length with respect to the number of relaxations.<sup>29</sup> For sufficiently long times, the thermodynamic speed is constant in a endoreversible quasi-static step system where the entropy production is minimum.<sup>28</sup>

The translation of this result to a continuous process is not straightforward and it has been causing some confusions in the past. Indeed, if one sees the continuous case as a step process with an infinite number of steps, by maintaining the above assumption of quasi-static equilibration steps, the reversible limit is found. This case is of no interest in this context, and the assumption of a quasi-static step process needs to be dropped. The results of equal thermodynamic speed (ETS) are thus not valid in continuous systems.

Using calculus of variations, Spirkel and Ries<sup>20</sup> showed that in a process where all forces can be controlled independently there is a quantity which is constant when the entropy production is minimum and the forces are differentiable once. With linear flux-force relations,

this constant quantity reduces to the local entropy production.<sup>20</sup> The speed that is constant in this case is the one measured by the metric given by the inverse of the matrix of Onsager coefficients.<sup>30,31</sup> Diosi et al.<sup>32</sup> clarified that constant thermodynamic speed, as measured with the Weinhold's metric, results from the entropy production minimization procedure when the optimization is carried out at a fixed number of relaxations instead of at a fixed time.

Continuous systems have often been approximated by quasi-static step processes with a finite number of steps, and the control strategy that yields minimum entropy production has been approximated by ETL between the steps.<sup>33,34</sup> The results obtained by imposing ETL have also been compared with the ones of the EoF method in a distillation column, as well as with the mathematical optimum.<sup>12,35</sup> The concept of ETS has been used to implement simulated annealing schedules.<sup>36-38</sup>

The main purpose of this work is to use some of the entropy production minimization results that have been presented in literature as design principles for minimization of entropy production, and to compare them to the numerical optimum. The goal is to establish under which circumstances they correspond to the numerical minimum, and, when they do not correspond, to establish their performances. A second purpose is to compare the results obtained with different equipartition principles. We shall use a membrane unit for separation of CO<sub>2</sub> from natural gas as an illustrative case. Such a system is quite simple, but, contrary to the heat exchanger example, it still allows to bring forward the importance of the number of controls on the process. Minimum entropy production in such system has already been studied in Ref.,<sup>39</sup> where the transport coefficient were assumed to be constant. Such an assumption is not made in the present work.

In Section 2, we present the two systems that are used to compare the procedures, while, in Section 3, we present a theoretical analysis on the equipartition results presented in literature. The solution procedure and the different cases which are investigated are illustrated in Section 4. After presenting the results in Section 5, we draw conclusions in Section 6.

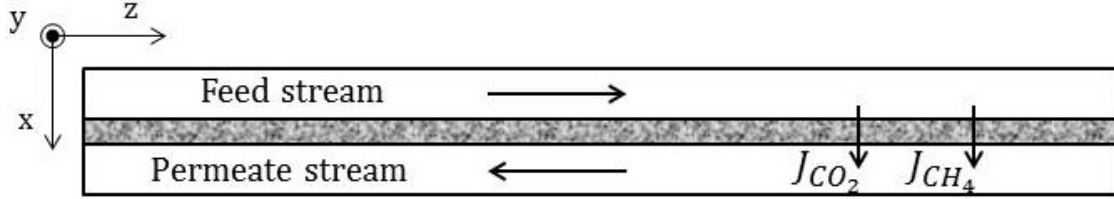


Figure 1: A schematic representation of the continuous separation system. The feed stream flows in the  $z$ -direction parallel to the membrane, which separate the feed and permeate streams. The component molar fluxes,  $J_{CO_2}$  and  $J_{CH_4}$ , cross the membrane perpendicularly to it ( $x$ -direction). The permeate stream,  $F^p$ , flows in opposite direction with respect to the feed,  $F^f$ .

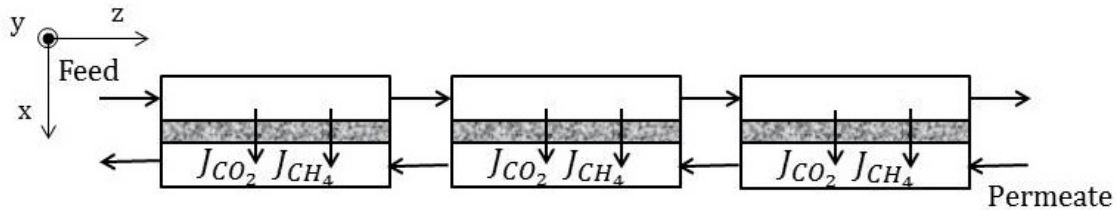


Figure 2: A schematic representation of the discrete separation system, with 3 stages. The natural gas to be treated is successively fed to the sequence of  $N = 3$  membrane units. The pressure on the permeate side might differ from one stage to another.

## 2 System

We reported in Section 1 that the entropy production minimization results found in the literature are different for continuous and discrete systems. Therefore, we consider a continuous and a discrete membrane system for  $CO_2$  separation from natural gas. In the first case, the system and the pressure profile on the permeate side are continuous, while in the second instance, they are staged. In both cases, the natural gas is assumed to be an ideal gas, and  $CO_2$  and methane are the only components considered in the natural gas.

### 2.1 Continuous membrane separation process

Figure 1 shows a schematic representation of the continuous system, which has been accurately described in Ref.<sup>39</sup> The feed stream flows from left to right, while the permeate flows parallel to the feed, but in opposite direction (counter-current fashion). Because of the difference in the component partial pressures between the two sides, fluxes of the two components

are established from feed to permeate. Since driving forces and transport coefficients are different, the two components permeate at different rates. Therefore, continuous gradients of the thermodynamic variables are present on both sides of the membranes ( $z$ -direction).

## 2.2 Discrete membrane separation process

Figure 2 shows a schematic representation of a discrete system with 3 stages. Each of the stages works as a continuous membrane system. After going through the first membrane stage, the feed gas is fed to the second stage, and so on. The permeate total pressure is constant inside each stage, but it varies between different stages. The permeate gas is fed to the membrane stages in a counter-current fashion with respect to the feed gas (from the stage at the far right to that to the far left). No full equilibration is reached between the two sides of the membrane.

## 3 Theoretical analysis

### 3.1 Entropy production and flux-force relations

The objective function of the thermodynamic optimization problem is the total entropy production of the system,  $\Sigma_{irr}$ . According to nonequilibrium thermodynamics,<sup>40</sup> the local entropy production of a homogeneous phase can be written as the product sum of all fluxes,  $J_i$ , and their conjugate forces,  $X_i$ . Fluxes and forces of interest in our system are related to mass transport of the two components across the membrane. The entropy production of a cross section of the system,  $\sigma$ , is:

$$\sigma = W \sum_i J_i X_i = W (J_{CO_2} X_{CO_2} + J_{CH_4} X_{CH_4}) \quad (1)$$



where  $W$  is the width of the membrane (in the  $y$ -direction). Here,  $i = \{\text{CO}_2, \text{CH}_4\}$ . Fluxes and forces can be related through a flux-force relation:

$$J_i = L_i X_i = -L_i \Delta \frac{\mu_i}{T} \quad (2)$$

where  $L_i$  is the component mass transport coefficient,  $\mu_i$  is the chemical potential, and  $T$  is the temperature. We use the symbol  $\Delta$  to indicate the difference between the permeate and the feed side. Since we consider the gas to be ideal, Eq. 2 can be rewritten as:

$$J_i = -RL_i \ln \frac{p^p x_i^p}{p^f x_i^f} \quad (3)$$

where  $R$  is the universal gas constant,  $p$  is the total pressure, and  $x_i$  is the component molar fraction. The superscripts  $p$  and  $f$  are used to indicate that a variable belongs to the permeate or feed side respectively. Introducing the flux-force relations given by Eq. 2 into Eq. 1, we obtain the local entropy production as a function of the driving forces only:

$$\begin{aligned} \sigma &= W \left( L_{\text{CO}_2} X_{\text{CO}_2}^2 + L_{\text{CH}_4} X_{\text{CH}_4}^2 \right) \\ &= W \left( L_{\text{CO}_2} \left( -\Delta \frac{\mu_{\text{CO}_2}}{T} \right)^2 + L_{\text{CH}_4} \left( -\Delta \frac{\mu_{\text{CH}_4}}{T} \right)^2 \right) \end{aligned} \quad (4)$$

In a continuous system, the total entropy production is the integral of the local entropy production over the total length of the membrane unit:

$$\begin{aligned} \Sigma_{irr} &= \int_0^L \sigma dz \\ &= W \int_0^L L_{\text{CO}_2} \left( -\Delta \frac{\mu_{\text{CO}_2}}{T} \right)^2 + L_{\text{CH}_4} \left( -\Delta \frac{\mu_{\text{CH}_4}}{T} \right)^2 dz \\ &= \Sigma_{irr, \text{CO}_2} + \Sigma_{irr, \text{CH}_4} \end{aligned} \quad (5)$$

where  $\Sigma_{irr, \text{CO}_2}$  and  $\Sigma_{irr, \text{CH}_4}$  are the contributions to entropy production given by the transport of  $\text{CO}_2$  and methane respectively.

Using optimal control theory, Johannessen and Kjelstrup<sup>17</sup> showed in a general way that, when the thermodynamic driving forces can be controlled independently and the flux-force relations are linear, the minimum in Eq. 5 is obtained when the argument of the integral and, thus, the local entropy production are constant. Calculus of variations<sup>16,29</sup> as well as other optimization tools<sup>41</sup> can also be used to prove this result. For a membrane unit, the EoEP has been analytically derived using optimal control theory in Ref.<sup>39</sup> In that work, EoF resulted from EoEP, since the transport coefficients and the proportionality coefficient matrix were constant.

When the driving forces cannot be controlled independently, the mathematical tools do not give information on the nature of the optimal solutions.

If the process takes place in discrete stages (Fig. 2), the entropy production of the whole system is given by the sum of the entropy produced in each of the  $N$  subsystems:

$$\Sigma_{irr}^{dis} = \sum_{n=1}^N \Sigma_{irr,n} = \sum_{n=1}^N \int_0^{L^{stage}} \sigma dz \quad (6)$$

where  $L^{stage}$  is the length of each membrane stage.

### 3.2 Thermodynamic length, speed, and entropy production

In finite-time thermodynamics, the dissipation of a process has been linked to its thermodynamic geometry. In particular, the thermodynamic distance, which is the distance between two thermodynamic states, is closely related to the system dissipation.

Weinhold<sup>27</sup> defined an equilibrium thermodynamic metric in terms of the extensive state variables and of the extensive entropy of the system,  $S^f$ . In the present case, the extensive variables are the component fluxes on the feed side,  $F_i^f$ , and the matrix is defined as:

$$g_{ik} = -\frac{\partial^2 S^f}{\partial F_i^f \partial F_k^f} \quad (7)$$

The intensive variables of the system can be expressed by:<sup>27</sup>

$$Y_i^f = \frac{\partial S^f}{\partial F_i^f} = -\frac{\mu_i^f}{T^f} \quad (8)$$

The thermodynamic length element,  $dl$ , is a function of the above thermodynamic metric and of the state variables according to:<sup>29</sup>

$$\begin{aligned} dl^2 &= \sum_{i,k} g_{ik} dF_i^f dF_k^f = -\sum_i dY_i^f dF_i^f \\ &= \sum_i d\left(\frac{\mu_i^f}{T^f}\right) dF_i^f \end{aligned} \quad (9)$$

With this formulation, the entropy production due to transfer of  $dF_i^f$  from feed to permeate can be formulated as:<sup>28</sup>

$$dS_u = -\sum_i \Delta Y_i dF_i^f \quad (10)$$

where  $\Delta$  indicates the difference between the permeate and the feed side. By substituting Eq. 8 into  $\Delta Y_i$ , and comparing it to the thermodynamic driving forces in Eq. 2, we find that  $\Delta Y_i = X_i$ . Even though the terms  $dY_i^f$  (in Eq. 9) and  $\Delta Y_i$  (in Eq. 10) look similar, they are different in nature, since they represent the infinitesimal change in the feed stream and the difference between the state of the permeate and the feed side respectively.

Equation 10 can be further elaborated by introducing the conservation equations into it (Eq. 22 in Appendix 6):

$$\begin{aligned} dS_u &= -\sum_i \Delta Y_i dF_i^f = -\sum_i X_i \frac{dF_i^f}{dz} dz \\ &= W \sum_i X_i J_i dz = \sigma dz \end{aligned} \quad (11)$$

Comparing Eqs. 1 and 11, we find that  $\sigma = dS_u/dz$ , and that, as expected, the two formulations are equivalent.

We now define the quantities:

$$\epsilon = \frac{dS_u/dz}{(dl/dz)^2} \quad (12)$$

$$d\xi = \frac{dz}{\epsilon} \quad (13)$$

$$\Xi = \int_0^L d\xi \quad (14)$$

where,  $\epsilon$  is a characteristic length. For sufficiently long processes,  $\epsilon$  corresponds to the relaxation length (or time, if time is the system coordinate). This is the only nonequilibrium parameter used in the finite-time formulation. Here,  $\xi$  is the number of relaxations which is a dimensionless quantity.<sup>29</sup>

The total entropy production is given by the integration of  $dS_u$  over the total membrane length,  $L$ ,<sup>29</sup>

$$\Sigma_{irr} = \int_0^L dS_u = \int_0^L \epsilon \left( \frac{dl}{dz} \right)^2 dz = \int_0^\Xi \left( \frac{dl}{d\xi} \right)^2 d\xi = \int_0^\Xi v_{TH}^2 d\xi \quad (15)$$

where  $v_{TH} = dl/d\xi$  is the thermodynamic speed. Reference<sup>29</sup> shows how calculus of variation can be used to prove that Eq. 15 is minimum when the argument of the integral and, thus,  $\sigma$  are constant. Even though it is not specified in Ref.,<sup>29</sup> in their derivation of EoEP, they assume to be able to independently control all driving forces. Moreover, the flux-force relations need to have a linear form, so that the entropy production can be written as:<sup>29</sup>

$$dS_u = \sum_i f(N_i) \left( \frac{dN_i}{dz} \right)^2 dz \quad (16)$$

where  $f(N_i)$  is a function of the state variables only.

If the optimization procedure is done ahead of the membrane unit design, the length of the membrane unit,  $L$ , can be a parameter of the optimization problem. In the particular case that  $L$  is free to vary, while the number of relaxations  $\Xi$  is fixed, it has been found that the entropy production is minimum when the argument of the integral in the last equality

of Eq. 15 is constant. Under this conditions, the thermodynamic speed is constant.<sup>32</sup>

The thermodynamic speed can be further elaborated to get:

$$\begin{aligned}
 v_{TH} &= \frac{dl}{d\xi} \\
 &= \frac{X_{CO_2}J_{CO_2} + X_{CH_4}J_{CH_4}}{\sqrt{\frac{R}{F^f x_{CO_2}^f x_{CH_4}^f} \left( J_{CO_2}x_{CH_4}^f - J_{CH_4}x_{CO_2}^f \right)^2}}
 \end{aligned} \tag{17}$$

The derivation of the last equality is presented in Appendix 6.

In a process that proceeds by discrete stages, when the steps are sufficiently short to consider the metric  $g_{ik}$  constant in every step, Eq. 9 can be integrated to obtain the thermodynamic length of the stage  $n$ :<sup>29</sup>

$$l_n = \sqrt{\sum_{i,k} g_{ik} \Delta_n F_i^f \Delta_n F_k^f} \tag{18}$$

where  $\Delta_n F_i^f$  is the difference in the state variable  $F_i^f$  between outlet and inlet of the stage  $n$ . The total thermodynamic length of the process will then be:

$$l = \sum_{n=1}^N l_n \tag{19}$$

If the metric  $g_{ik}$  can be considered constant in every step of the process, the total entropy production is minimum when the steps are spaced such that the thermodynamic distance between them is the same.<sup>42</sup>

When the metric  $g_{ik}$  cannot be considered constant, the thermodynamic length of a step is found by integrating Eq. 29 over the length of the step,  $L^{stage}$ .

## 4 Calculation details

In order to establish a reference, the entropy production of a membrane system with constant permeate pressure is calculated. In this case, the state variables' profiles are found by integrating the component conservation equations presented in Appendix 6 (Eq. 22). Since the permeate feed at the outlet of the membrane is needed to calculate the permeate flows at any position (Eq. 23), the problem is solved by using the Matlab “bvp4c” solver, which is a collocation method that allows the integration of ordinary differential equations, where a set of constant parameters is unknown. Here,  $F^{f,out}$  is set as the unknown parameter.

The entropy production and the thermodynamic profiles for the controlled cases are found through a numerical minimization procedure. We used the Matlab optimization function “fmincon”, which is a nonlinear programming solver that allows us to find the minimum of an objective function subject to equality and inequality constraints. The total entropy production described by Eq. 5 (or, equivalently, by Eq. 15) is set as the objective function of the optimization problem.

The equality constraints are given by inlet feed and permeate flows, by the governing equations (Eqs. 22), and by a constraint on the separation duty of the membrane unit:

$$x_{CO_2}^{f,out} = 0.02 \tag{20}$$

When later in this section we impose the entropy production minimization results on the system, a further constraint is needed (See Sec. 4.2).

Some inequality constraints are also imposed to prevent the numerical solver to choose unfeasible solutions for the problem. Since we want the component fluxes across the membrane to be directed from the feed to the permeate side, the  $N_i^f$  should not be larger than the ones at an earlier position along the membrane. Moreover, the permeate pressure needs to be positive.

Since the numerical solver does not guarantee that the minimum that is found is a global

Table 1: Operating conditions for the reference membrane process.<sup>43</sup> In the reference process, the pressure on both sides are constant along the  $z$ -direction. The same constant temperature is considered at the two sides of the membrane. A sweep gas with the same composition as the natural gas to be treated is used on the permeate side.

	Value	Units
$T$	308	K
$p^f$	$50 \cdot 10^5$	Pa
$p^p$	$1 \cdot 10^5$	Pa
$F^{f,in}$	0.098	$\text{mol} \cdot \text{s}^{-1}$
$F^{p,in}$	0.002	$\text{mol} \cdot \text{s}^{-1}$
$x_{CO_2}^{f,in}$	0.3	-
$x_{CO_2}^{p,in}$	0.3	-
$W$	1	m
$L$	57.6	m

minimum, we repeat the numerical calculations several times, with different random initial profiles for the state and control variables. When the results converge to the same solution, we assume that the global minimum is found.

## 4.1 Relevant data

Calculations are performed at a typical set of operating conditions for purification of natural gas. Table 1 reports the main relevant data used in calculations. In the reference case, the total pressure is constant on both sides of the membrane, since we neglect the pressure drop due to viscous flow. However, a large pressure drop is present between the two sides of the membrane unit. Since there are no heat sources and the gas is considered to be ideal, the temperature results to be constant across the system.<sup>44</sup> In order to meet pipeline specifications,<sup>43</sup> the total length of the membrane unit ( $L$ ) is chosen so that the  $CO_2$  content of the treated natural gas is 2% at the exit of the reference membrane process. The permeability data in Ref.<sup>45</sup> are used to derive the variable transport coefficients. The coefficients  $L_i$  (Eq. 2) are functions of the feed composition.

## 4.2 Investigated cases

In order to establish the conditions for validity of the entropy production minimization results that are derived in literature, and to evaluate their performances as entropy production minimization designs, we compare the entropy production obtained in different cases:

**Reference case (Ref):** In the reference case, the total pressure on the permeate side is constant.

**Numerical optimum (NumOpt):** The partial or total pressures on the permeate side are continuously controlled so that the total entropy production of the process is minimum and the equality constraints given earlier in Section 4 are satisfied.

**Equipartition of entropy production (EoEP):** The total entropy production is minimized with the additional constraint that the local entropy production needs to be constant. The constant value of the local entropy production is a parameter of the optimization procedure.

**Equipartition of forces (EoF):** The total entropy production is minimized with the additional constraint that the thermodynamic driving forces need to be constant. When we can control the permeate partial pressures, it is possible to make both driving forces constant. When we can control only the permeate total pressure, we can force just one driving force to be constant. Therefore, we will impose separately constant driving force to CO<sub>2</sub> transport (EoF<sub>CO<sub>2</sub></sub>) or constant driving force to methane transport (EoF<sub>CH<sub>4</sub></sub>).

**Equal thermodynamic speed (ETS):** The total entropy production is minimized with the additional constraint that the thermodynamic speed needs to be constant.

In all the cases mentioned above (with exception for the reference case), we assume that we are able to control the permeate partial or total permeate pressure at any position. When we can control both component partial pressures, the driving forces can be controlled



Table 2: Total entropy production of the continuous membrane unit for the reference case (Ref), and in the cases where 2 variables are controlled (NumOpt, EoEP, EoF, and ETS). The percentage in parenthesis represents the fraction of the possible entropy production reduction which is obtained, calculated according to Eq. 21.

$\text{J}\cdot\text{K}^{-1}\cdot\text{s}^{-1}$	Ref	NumOpt	EoEP	EoF	ETS
$\Sigma_{irr}$	0.958	0.483	0.483 (100%)	0.520 (92.2%)	0.500 (96.2%)
$\Sigma_{irr,CO_2}$	0.602	0.483	0.483	0.520	0.497
$\Sigma_{irr,CH_4}$	0.356	$1.6 \cdot 10^{-4}$	$1.6 \cdot 10^{-4}$	$3.2 \cdot 10^{-5}$	0.003

independently. On the other hand, the control of the total pressure only does not allow us to have such freedom of control.

Since some of the equipartition results presented in literature are derived for discrete processes, we also consider a staged membrane unit, where the total permeate pressure is controlled in every stage. In the discrete case, we compare the following cases:

**Numerical optimum (NumOpt):** We find the permeate total pressures that needs to be assigned to every stage in order to minimize the total entropy production, while satisfying the equality constraints given above.

**Equipartition of entropy production (EoEP):** We minimize the total entropy production with the additional constraint that the total entropy production of the stage is the same for all stages.

**Equal thermodynamic length (ETL):** We minimize the total entropy production with the additional constraint that the thermodynamic length of every stage is the same for all stages.

**Equal thermodynamic length from Eq. 18 (ETL approx):** We minimize the total entropy production with the additional constraint that the thermodynamic length of every stage calculated according to Eq. 18 is the same for all stages.

## 5 Results and discussion

### 5.1 Continuous process

In this section, we present and compare the results obtained by applying the equipartition results to the continuous reference process. First, we compare the results obtained when we can control all driving forces independently. We then analyze the case in which the control on the system is not sufficient to drive the forces independently.

#### 5.1.1 Independent control of all driving forces

In order to control all driving forces, we need to have control on a number of variables that is equal or larger than the number of independent state variables.<sup>17</sup> The assumption of being able to independently control all driving forces is needed to derive all the equipartition results analyzed in Section 3. For a membrane unit, the control of the permeate partial pressures represents a possible way to achieve this kind of control. Other choices are possible. However, as long as the choice of control variables enables us to control the driving forces independently, the results are not influenced by this choice.

When we control the permeate partial pressures, we implicitly control the permeate composition at every position. Thus, the component mass balances on the permeate side which are given by Eq. 23 are not obeyed.

Table 2 presents the total entropy production in the investigated cases, as well as the contributions to it given by transport of the different components. In the optimal numerical case (NumOpt), the total entropy production is reduced by 49.6% with respect to the reference case (Ref). The entropy production due to methane transport is not exactly zero in the optimal case, however, it is several orders of magnitude smaller than the one due to CO<sub>2</sub> transport. The reduction of  $\Sigma_{irr,CH_4}$  gives the largest contribution to the total entropy production reduction.

The percentage in parenthesis represents the fraction of the possible entropy production

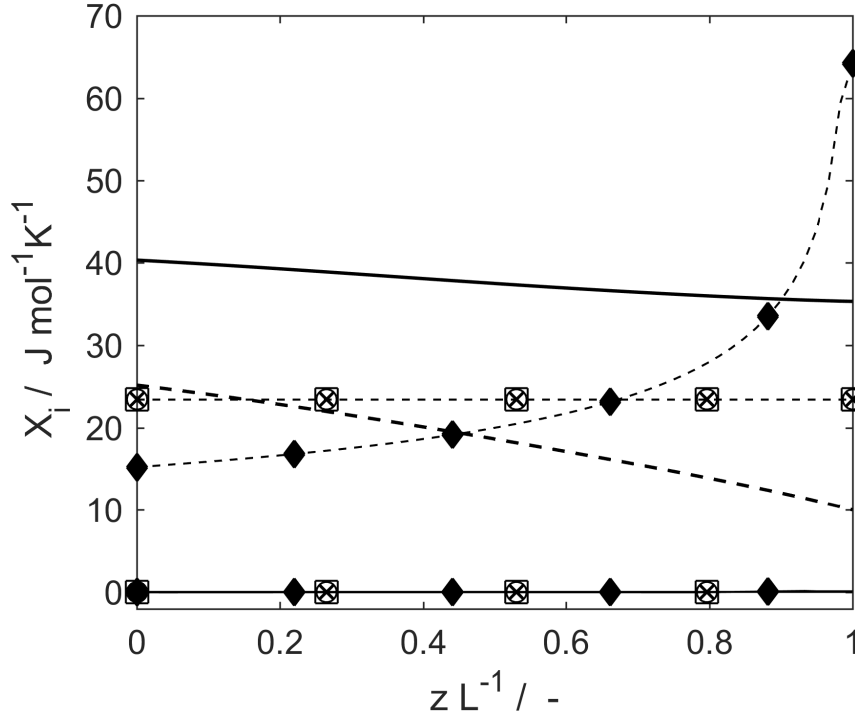


Figure 3: Thermodynamic driving force to CO<sub>2</sub> transport (dashed lines) and methane transport (solid lines) of the continuous membrane unit for the reference case (thick lines), and for the cases where 2 variables are controlled (× for NumOpt, ○ for EoEP, □ for EoF, and ◆ for ETS). The ×, ○ and □ symbols coincide. The transport coefficients are constant.

reduction which is obtained when the equipartition results are used as design principles.

Such fraction is calculated as:

$$\% = \frac{\Sigma_{irr}^{Ref} - \Sigma_{irr}}{\Sigma_{irr}^{Ref} - \Sigma_{irr}^{NumOpt}} \cdot 100 \quad (21)$$

where  $\Sigma_{irr}$  is the entropy production in the considered case, and  $\Sigma_{irr}^{Ref}$  is the entropy production in the reference case. Here, we use  $\Sigma_{irr}^{NumOpt}$  to indicate the entropy production of the NumOpt considered in this section. Table 2 shows that the entropy production obtained with EoEP equals that of the optimal case (by the numerical accuracy of the calculations,  $10^{-6}$ ). This result is in agreement with the theoretical analysis conducted in Section 3. Indeed, the conditions for derivation of EoEP are satisfied (i.e. independent control of the driving forces, linear flux-force relations, and  $\sigma$  not explicitly dependent on the spatial coordinate  $z$ ).

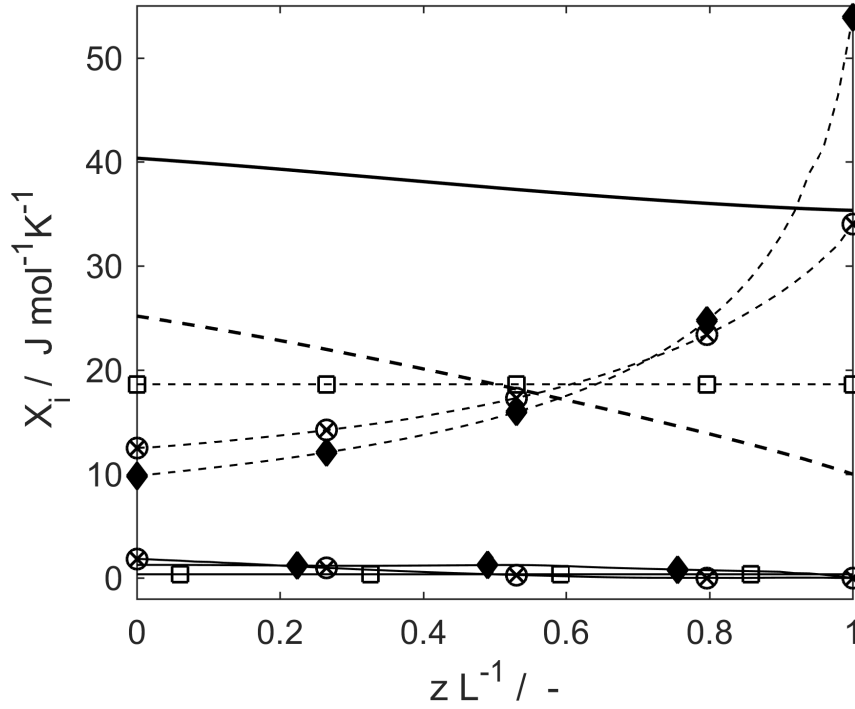


Figure 4: Thermodynamic driving force to CO<sub>2</sub> transport (dashed lines) and methane transport (solid lines) of the continuous membrane unit for the reference case (thick lines), and in the cases where 2 variables are controlled (× for NumOpt, ○ for EoEP, □ for EoF, and ◆ for ETS). The × and ○ symbols coincide. The transport coefficients are functions of the state variables.

On the other hand, EoF does not coincide with the optimum. Equipartition of forces characterizes the optimal solution under two different sets of assumptions. In the first case, any variation in the state variables needs to be allowed, even the unfeasible ones. By obeying the conservation equations on the feed side, we do not satisfy this condition. In the second case, EoF follows from EoEP if the transport coefficients and the proportionality factor matrix of the optimal control theory formulation are constant.<sup>17</sup> In the present case, the proportionality factor matrix is constant. However, the transport coefficients are functions of the feed composition, and thus the conditions are not satisfied. We can verify this last case by running the same calculations with constant transport coefficients. Figure 3 shows that, when the transport coefficients are constant, the thermodynamic driving force profiles of NumOpt (× symbols), EoEP (○ symbols) and EoF (□ symbols) coincide at the numerical

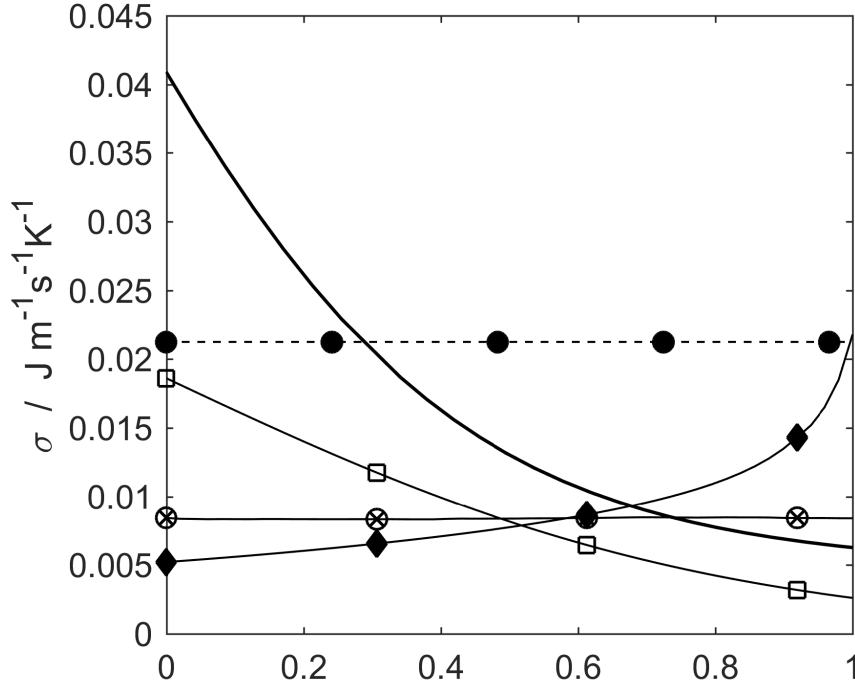


Figure 5: Local entropy production of the continuous membrane unit for the reference case (thick solid line), and in the cases where 2 variables are controlled ( $\times$  for NumOpt,  $\circ$  for EoEP,  $\square$  for EoF, and  $\blacklozenge$  for ETS). The  $\times$  and  $\circ$  symbols coincide. The  $\bullet$  symbols represent a case where  $\sigma$  is constant but  $\Sigma_{irr}$  is not minimized.

accuracy of the calculations ( $10^{-6}$ ). The same results were found in Ref.,<sup>39</sup> where constant transport coefficients were used. However, EoF gives a good approximation of the minimum even when it does not correspond to it, as it allows for 92.2% of the maximum entropy production reduction (Table 2).

Equal thermodynamic speed ( $\blacklozenge$  symbols) does not coincide with the optimum. Indeed, ETS coincides with the optimal solution only when the optimization is carried out at fixed number of relaxation,  $\Xi$ , instead of fixed length of the membrane unit, and under the same conditions necessary to obtain EoEP (i.e. independent control of the driving forces, linear flux-force relations, and  $\sigma$  not explicitly dependent on the spatial coordinate  $z$ ). Since the membrane length is fixed, these conditions are not satisfied. Nonetheless, ETS approximates the minimum very well, as it allows for 96.2% of the maximum entropy production reduction (Table 2).

Figure 4 depicts the thermodynamic driving forces to transport of CO<sub>2</sub> (dashed lines) and methane (solid lines), for transport coefficients that are functions of the state variables. In this case only NumOpt (× symbols) and EoEP (○ symbols) coincide. The driving force profiles are quite different in the different cases. However, the deviations in total entropy production of EoF and ETS with respect to NumOpt and EoEP are quite small (Table 2). Thus, it seems that, also for membrane systems, the entropy production minimum in the thermodynamic space is quite flat and, therefore, relatively large perturbations from the optimal profiles result in small differences in the total entropy production.<sup>12,16</sup>

When the permeate partial pressures are controlled, the entropy production is mostly due to the transport of CO<sub>2</sub> (Table 2). Figure 4 shows that, in the first part of the membrane, all equipartition methods make the CO<sub>2</sub> driving force smaller than in the reference case, while, in the second part, they make it larger. Thus, to some extent, all equipartition principles move in the same direction. However, EoF (□ symbols) does not reduce enough the driving force in the first part of the membrane, while it enlarges it too little in the second part (cf. with the optimal case, × symbols). In contrast, ETS (◆ symbols) has opposite behavior. The optimal driving forces are always between those of EoF and those of ETS.

The total entropy production is the integral of the local entropy production over the membrane unit. In Fig. 5, we can see that the  $\sigma$  obtained by imposing EoF (□ symbols) deviates from the optimal one (× symbols) in a positive manner in the first half of the membrane, while it has a negative deviation in the second half. Overall, the two deviations cancel each other for the largest part, resulting in a small total entropy production difference from the optimal case. For the case where ETS is imposed (◆ symbols), the deviations from the optimal local entropy production are opposite to those obtained with EoF. However, also in this case the two deviations mostly cancel each other.

An optimization procedure is still necessary to obtain the EoEP, EoF and ETS results that we have presented in this section. Indeed, in the present case, different partial pressure profiles can give constant local entropy production (or constant driving forces, or constant

Table 3: Total entropy production of the continuous membrane unit for the reference case (Ref), and in the cases where 1 variable is controlled (NumOpt, EoEP, EoF<sub>CO<sub>2</sub></sub>, EoF<sub>CH<sub>4</sub></sub>, and ETS). The percentage in parenthesis represents the fraction of the possible entropy production reduction which is obtained, calculated according to Eq. 21.

$\text{J}\cdot\text{K}^{-1}\cdot\text{s}^{-1}$	Ref	NumOpt	EoEP	EoF <sub>CO<sub>2</sub></sub>	EoF <sub>CH<sub>4</sub></sub>	ETS
$\Sigma_{irr}$	0.958	0.838	0.841(97.2%)	0.868(75.3%)	0.919(32.6%)	0.844(95.3%)
$\Sigma_{irr,CO_2}$	0.602	0.478	0.484	0.514	0.565	0.478
$\Sigma_{irr,CH_4}$	0.356	0.360	0.357	0.354	0.354	0.366

thermodynamic speed), without being the optimal ones. As an example, the ● symbols in Fig. 5 show a case where the local entropy production is constant, but where the total entropy production is not minimum. In the example, the total entropy production is even larger than that of the reference case ( $\Sigma_{irr} = 1.22 \text{ J}\cdot\text{K}^{-1}\cdot\text{s}^{-1}$ ). However, even if the optimization procedure is still needed, the optimization problem reduces in complexity since the optimization is carried out with only one scalar to be determined (the equipartitioned quantity), instead of the unknown profiles of the two control variables.

This phenomenon is due to the fact that the number of constraints on the process (i.e. the inlet molar flows,  $F_i^{f,in}$ , and the separation duty given by Eq. 20) is smaller than the total number of state and control variables. Thus, more than one system design might correspond to each of the equipartition results. When the number of constraints and the total number of state and control variables are the same, the solution is unique, and the optimization procedure is not necessary. For the present case, it is possible to obtain the same number of constraints and the total number of state and control variables by adding a constraint to the process (for instance, we could impose the methane losses to be zero,  $F_{CH_4}^{f,out} = F_{CH_4}^{f,in}$ ). However, the additional constraint limits to some degree the possibility to reduce the entropy production.

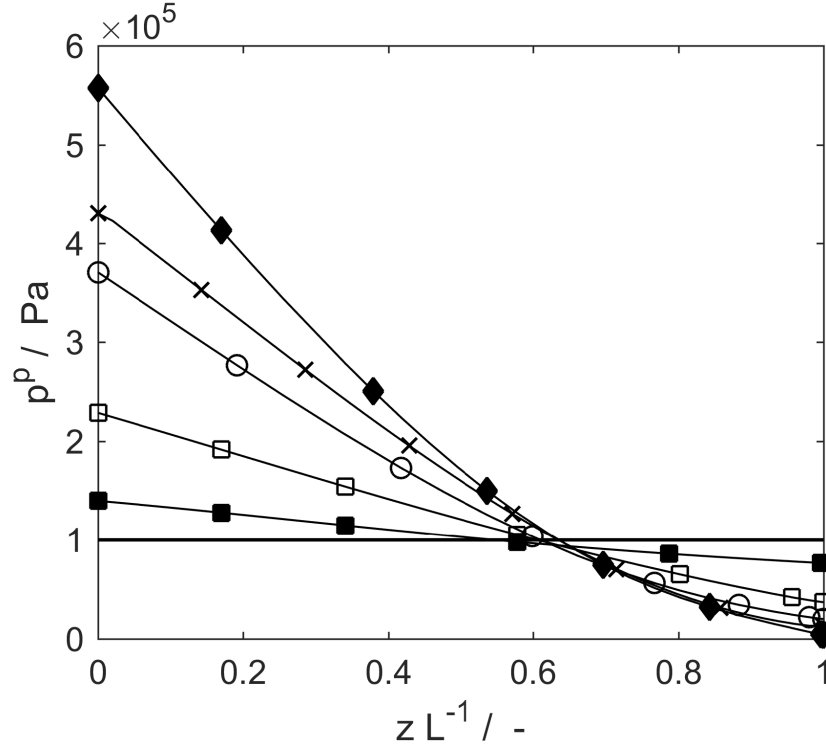


Figure 6: Permeate pressure in the continuous membrane unit for the reference case (solid thick line), and in the cases where 1 variable is controlled ( $\times$  for NumOpt,  $\circ$  for EoEP,  $\square$  for EoF<sub>CO<sub>2</sub></sub>,  $\blacksquare$  for EoF<sub>CH<sub>4</sub></sub>, and  $\blacklozenge$  for ETS).

### 5.1.2 Partial control of the driving forces

When we control the total permeate pressure only, the driving forces cannot be controlled independently. According to the analysis in Section 3, without independent control of all driving forces, none of the equipartition results can be analytically derived.

Other choices of the control variable are possible and, in this case, a different choice of the control would lead to different results of the optimization process.

Table 3 presents the total entropy production in the investigated cases, as well as the contributions to it given by transport of the different components. With the control of the total permeate pressure only, the reduction in the total entropy production is much smaller than the one obtained by having control of all driving forces. In the optimal numerical case (NumOpt), the total entropy production is reduced by only 12.5% with respect to the reference case (Ref). The overall reduction in entropy production is due to the reduction



in  $\Sigma_{irr,CO_2}$  only, while  $\Sigma_{irr,CH_4}$  is slightly increased. Similarly, in Ref.,<sup>46</sup> it was found that the reduction in entropy production in an optimally controlled steam reformer was only due to the reduction of one of its contributions, while all the other contributions had slightly increased.

The percentage in parenthesis represents the fraction of the possible entropy production reduction which is obtained when the equipartition results are used as design principles. The percentages are calculated according to Eq. 21, where we now use the entropy production of the NumOpt considered in this section. Table 3 shows that neither of the equipartition results (EoEP, EoF<sub>CO<sub>2</sub></sub>, EoF<sub>CH<sub>4</sub></sub>, and ETS) coincides with the optimum. Nevertheless, imposing EoEP and ETS approximates well the optimum, by bringing the total entropy production circa 97.2% and 95.3% towards the minimum, respectively. EoF<sub>CO<sub>2</sub></sub> does not perform as well as EoEP and ETS, as it allows for only 75.3% of the reduction in entropy production obtained in NumOpt.

Figure 6 shows how the permeate pressure is operated in the different investigated cases. EoEP (○ symbols) and ETS (◆ symbols) approximate quite well the optimal pressure profile (× symbols) close to the end of the membrane unit. However, they have larger deviations from the optimal solution in the first half of the membrane unit. The optimal pressure profile is everywhere included between the profiles obtained by imposing EoEP and ETS.

Differently from the case analyzed in Sec. 5.1.1, the permeate pressure profiles obtained by imposing the equipartition results are uniquely determined in this case. Indeed, the number of constraints equals the total number of state and control variables. Therefore, the optimization procedure is not necessary in the present case.

Since EoEP and ETS give very good approximations of the optimum (Table 3), they can be used as design principles to reduce entropy production in CO<sub>2</sub> separation membrane processes.

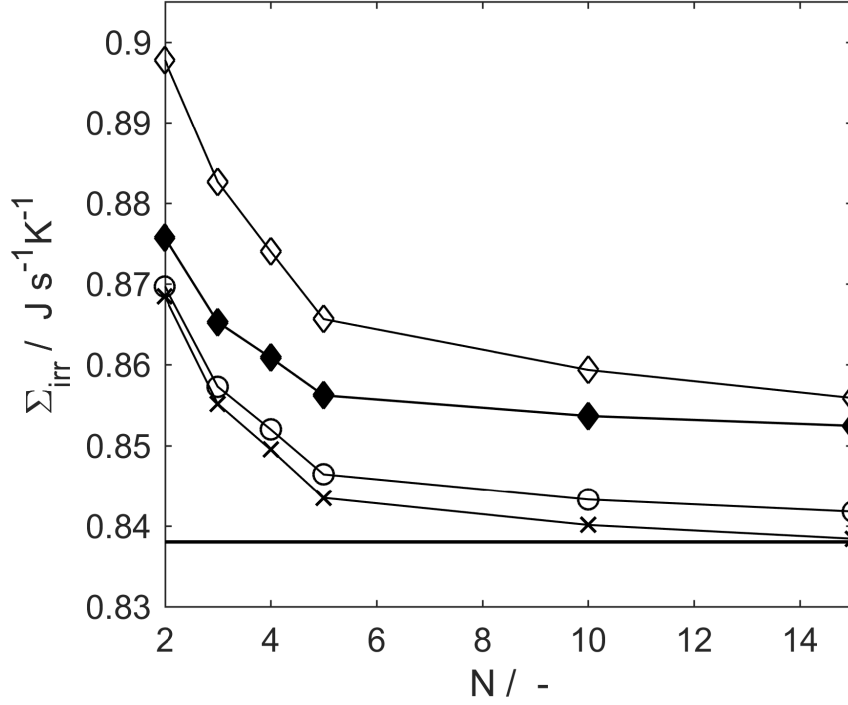


Figure 7: Total entropy production of the staged membrane as function of the number of stages,  $N$ . We use  $\times$  for NumOpt,  $\circ$  for EoEP,  $\blacklozenge$  for ETL, and  $\diamond$  for ETL approx. The thick solid line shows  $\Sigma_{irr}$  for the continuous NumOpt case.

## 5.2 Discrete process

Some of the equipartition results discussed in Section 3 have been derived for processes where the system proceeds through a series of stages. In this section, we present and compare the results obtained by applying the equipartition results to a discrete membrane process.

We assume that we can control the total permeate pressure at the inlet of every stage, and we compare the results obtained for different number of stages. The total length of the membrane unit is the same in every case ( $L$ ), and the length of every stage is simply  $L^{stage} = L/N$ . Thus, the stage lengths are not parameters of the optimization problem.

Figure 7 reports the total entropy production obtained with NumOpt ( $\times$  symbols), EoEP ( $\circ$  symbols), ETL ( $\blacklozenge$  symbols), and ETL approx ( $\diamond$  symbols), as functions of the number of stages,  $N$ . The thick solid line shows the numerical optimal continuous results obtained in Section 5.1.2. As it is reasonable to expect, the NumOpt approaches the continuous optimum

as the number of stages increases.

None of the equipartition results coincides with the optimum. However, EoEP ( $\circ$  symbols) gives the best approximation of it. As the number of stages increases, the results obtained with EoEP approach those obtained in the EoEP continuous case (see Table 3).

Also ETL( $\blacklozenge$  symbols) approximates well the solution for low numbers of stages, while its performance is less good at higher numbers of stages. The reason why ETL does not coincide with the minimum is that one of the conditions to obtain the ETL results is not satisfied in the present system. Indeed, in order to derive ETL, it is necessary that the system (gas on the feed side) equilibrates with the ambient (gas on the permeate side) in every step of the discrete process. This condition is not satisfied in the discrete membrane unit. A comparison with Table 3 shows that ETL does not converge to ETS when  $N$  increases.

The comparison between the results obtained with ETL ( $\blacklozenge$  symbols) and ETL approx ( $\blacklozenge$  symbols) shows that to consider the metric  $g_{ik}$  constant in every stage is not a good approximation when the number of stages is small. The two results converge for increasing number of stages.

## 6 Conclusions

We have in this work analyzed and compared some of the different results of entropy production minimization procedures on optimally controlled systems that have been presented in literature. After listing the assumptions made in their derivation, we have used the results as design principles for entropy production reduction in a membrane unit for  $\text{CO}_2$  separation from a  $\text{CO}_2$ /methane mixture, and compared them to the numerically determined optimum. In the considered example, the flux-force relations were linear and the local entropy production was not an explicit function of the spatial coordinate.

For a continuous process, we considered and compared the equipartition of forces (EoF), the equipartition of entropy production (EoEP), and the equal thermodynamic speed (ETS)

results. When all driving forces were controlled independently, the numerical optimum and EoEP coincided. With the further assumption of constant transport coefficients, EoF corresponded to EoEP and numerical optimum. ETS coincides with the optimal solution only when the optimization is carried out at fixed number of relaxations, instead of fixed length of the membrane unit. Even though EoF and ETS did not give the numerical optimum, they approximated it well.

When the thermodynamic driving forces could not be controlled independently, none of the equipartition results characterized the optimal solution. However, EoEP and ETS approximated the optimum very well.

With or without the ability to independently control the driving forces, EoEP and ETS gave good approximations of (or coincided with) the numerical optimum. Thus, they can be used as design principles to reduce entropy production in CO<sub>2</sub> separation membrane systems. However, we showed that one should be careful, when the number of constraints imposed on the system is smaller than the total number of state and control variables. Under these circumstances, more than one solution might be compatible with the equipartition results, and, thus, the optimization procedure is still needed. Nonetheless, the use of equipartition results greatly reduces the complexity of the optimization problem. When the number of constraints equals the total number of state and control variables, the solution to the equipartition principles is unique.

For a discrete process, we considered and compared the EoEP, the equal thermodynamic length (ETL), and the approximated equal thermodynamic length (ETL approx) results. We assumed to be able to control the permeate total pressure in every stage. None of the equipartition results coincided with the numerical optimum. However, EoEP gave the best approximation of the discrete optimum, especially for low numbers of stages. Since the process was not an equilibration process, ETL did not coincide with the optimum, but still approximated it well. Finally, ETL approx was not a good approximation of ETL for small numbers of stages.

# Appendix

## Thermodynamic length and speed for a membrane system

### Conservation equations

On the feed side, the molar balance of component  $i$  for a cross section of the system on the  $xy$ -plane can be written as

$$\frac{dF_i^f}{dz} = -W J_i \quad (22)$$

The component flows on the permeate side can be calculated at all positions as:

$$F_i^p = F_i^{p,in} + (F_i^{f,out} - F_i^f) \quad (23)$$

### The thermodynamic metric $g_{ik}$

Equation 7 gives an expression for the thermodynamic metric  $g_{ik}$  in terms of the second derivatives of the extensive entropy with respect to the state variables. In this subsection, we will derive the  $g_{ik}$  for the specific case.

In the present system, we consider the feed component molar flows,  $F_i^f$ , as independent state variables. The first derivative of  $S^f$  with respect of the  $F_i^f$  is given by the component chemical potential over the temperature (Eq. 8). Thus, the second derivative with respect to  $F_{CO_2}^f$  is:

$$\begin{aligned} g_{CO_2CO_2} &= -\frac{\partial^2 S^f}{\partial (F_{CO_2}^f)^2} = \frac{\partial}{\partial F_{CO_2}^f} \left( \frac{\mu_{CO_2}^f}{T^f} \right) \\ &= \frac{\partial}{\partial F_{CO_2}^f} \left( \frac{\mu_{CO_2}^{ref}}{T^f} + R \ln \frac{p^f x_{CO_2}^f}{p^{ref}} \right) \\ &= R \frac{x_{CH_4}^f}{F_{CO_2}^f} \end{aligned} \quad (24)$$

where  $\mu_{CO_2}^{ref}$  is the component chemical potential in the reference state, and  $p^{ref}$  is the pressure

of the reference state. Similarly, we get:

$$\begin{aligned}
g_{CH_4CH_4} &= -\frac{\partial^2 S^f}{\partial (F_{CH_4}^f)^2} = \frac{\partial}{\partial F_{CH_4}^f} \left( \frac{\mu_{CH_4}^f}{T^f} \right) \\
&= \frac{\partial}{\partial F_{CH_4}^f} \left( \frac{\mu_{CH_4}^{ref}}{T^f} + R \ln \frac{p^f x_{CH_4}^f}{p^{ref}} \right) \\
&= R \frac{x_{CO_2}^f}{F_{CH_4}^f}
\end{aligned} \tag{25}$$

and:

$$\begin{aligned}
g_{CO_2CH_4} &= -\frac{\partial^2 S^f}{\partial F_{CO_2}^f \partial F_{CH_4}^f} = \frac{\partial}{\partial F_{CO_2}^f} \left( \frac{\mu_{CH_4}^f}{T^f} \right) \\
&= \frac{\partial}{\partial F_{CO_2}^f} \left( \frac{\mu_{CH_4}^{ref}}{T^f} + R \ln \frac{p^f x_{CH_4}^f}{p^{ref}} \right) \\
&= -R \frac{1}{F^f}
\end{aligned} \tag{26}$$

### Thermodynamic length

The thermodynamic length was defined in Section 3.2 as:

$$dl^2 = \sum_{i,k} g_{ik} dF_i^f dF_k^f \tag{27}$$

By expanding the summation and substituting Eq. 22 and Eqs. 24-26 into Eq. 27, we get:

$$\begin{aligned}
dl^2 &= R \frac{x_{CH_4}^f}{F_{CO_2}^f} (dF_{CO_2}^f)^2 - R \frac{2}{F^f} dF_{CO_2}^f dF_{CH_4}^f + R \frac{x_{CO_2}^f}{F_{CH_4}^f} (dF_{CH_4}^f)^2 \\
&= R \frac{(x_{CH_4}^f dF_{CO_2}^f - x_{CO_2}^f dF_{CH_4}^f)^2}{F^f x_{CO_2}^f x_{CH_4}^f} \\
&= W^2 R \frac{(x_{CO_2}^f J_{CH_4}^f - x_{CH_4}^f J_{CO_2}^f)^2}{F^f x_{CO_2}^f x_{CH_4}^f} dz^2
\end{aligned} \tag{28}$$

Thus, the infinitesimal thermodynamic length can be written as:

$$dl = W \sqrt{R \frac{\left(x_{CO_2}^f J_{CH_4}^f - x_{CH_4}^f J_{CO_2}^f\right)^2}{F^f x_{CO_2}^f x_{CH_4}^f}} dz \quad (29)$$

### Thermodynamic speed

The thermodynamic speed was defined in Section 3.2 as:

$$v_{TH} = \frac{dl}{d\xi} = \epsilon \frac{dl}{dz} \quad (30)$$

Introducing Eqs. 29 and Eq. 12 into Eq. 30, we get:

$$\begin{aligned} v_{TH} &= \frac{dS_u/dz}{(dl/dz)^2} \frac{dl}{dz} \\ &= \frac{\sigma}{dl/dz} \\ &= \frac{\sigma}{W \sqrt{R \frac{\left(x_{CO_2}^f J_{CH_4}^f - x_{CH_4}^f J_{CO_2}^f\right)^2}{F^f x_{CO_2}^f x_{CH_4}^f}}} \end{aligned} \quad (31)$$

## Acknowledgement

The project is funded by VISTA - a basic research program in collaboration with The Norwegian Academy of Science and Letters, and Statoil.

## References

- (1) Gouy, G. Sur l'énergie utilisable. *J. Phys.* **1989**, *8*, 501–518.
- (2) Hoffmann, K. H.; Andresen, B.; Salamon, P. Measures of dissipation. *Phys. Rev. A* **1989**, *39*, 3618.

- (3) Badescu, V. Optimal paths for minimizing lost available work during usual finite-time heat transfer processes. *J. Non-Equilib. Thermodyn.* **2004**, *29*, 53–73.
- (4) Tondeur, D.; Kvaalen, E. Equipartition of entropy production. An optimality criterion for transfer and separation processes. *Ind. Eng. Chem. Res.* **1987**, *26*, 50–56.
- (5) Salamon, P.; Nitzan, A.; Andresen, B.; Berry, R. S. Minimum entropy production and the optimization of heat engines. *Phys. Rev. A* **1980**, *21*, 2115.
- (6) Sauar, E.; Kjelstrup Ratkje, S.; Lien, K. M. Equipartition of forces: a new principle for process design and optimization. *Ind. Eng. Chem. Res.* **1996**, *35*, 4147–4153.
- (7) Bedeaux, D.; Standaert, F.; Hemmes, K.; Kjelstrup, S. Optimization of processes by equipartition. *J. Non-Equilib. Thermodyn.* **1999**, *24*, 242–259.
- (8) Nummedal, L.; Kjelstrup, S. Equipartition of forces as a lower bound on the entropy production in heat exchange. *Int. J. Heat Mass Transfer* **2001**, *44*, 2827–2833.
- (9) Balkan, F. Comparison of entropy minimization principles in heat exchange and a shortcut principle: EoTD. *Int. J. Energy Res.* **2003**, *27*, 1003–1014.
- (10) Ratkje, S. K.; Sauar, E.; Hansen, E. M.; Lien, K. M.; Hafskjold, B. Analysis of entropy production rates for design of distillation columns. *Ind. Eng. Chem. Res.* **1995**, *34*, 3001–3007.
- (11) Sauar, E.; Kjelstrup Ratkje, S.; Lien, K. Process optimization by equipartition of forces. Applications to distillation columns. *Efficiency, Costs, Optimization, Simulation and Environmental Impact of Energy Systems* **1995**, *2*, 413–418.
- (12) Sauar, E.; Siragusa, G.; Andresen, B. Equal thermodynamic distance and equipartition of forces principles applied to binary distillation. *J. Phys. Chem. A* **2001**, *105*, 2312–2320.



- (13) Sauar, E.; Kjelstrup, S.; Lien, K. M. Equipartition of forces – extension to chemical reactors. *Comput. Chem. Eng.* **1997**, *21*, S29–S34.
- (14) Kjelstrup, S.; Sauar, E.; Bedeaux, D.; Kooi, H. Reactor design by the principle of equipartition of forces and its extensions. *Zesz. Nauk. Politech. Świąt., Mech.* **1998**, 133–145.
- (15) Sauar, E.; Nummedal, L.; Kjelstrup, S. The principle of equipartition of forces in chemical reactor design: The ammonia synthesis. *Comput. Chem. Eng.* **1999**, *23*, S499–S502.
- (16) Johannessen, E.; Nummedal, L.; Kjelstrup, S. Minimizing the entropy production in heat exchange. *Int. J. Heat Mass Transfer* **2002**, *45*, 2649–2654.
- (17) Johannessen, E.; Kjelstrup, S. A highway in state space for reactors with minimum entropy production. *Chem. Eng. Sci.* **2005**, *60*, 3347–3361.
- (18) Bejan, A. Entropy generation minimization: The new thermodynamics of finite-size devices and finite-time processes. *J. Appl. Phys.* **1996**, *79*, 1191–1218.
- (19) Andresen, B.; Gordon, J. Optimal paths for minimizing entropy generation in a common class of finite-time heating and cooling processes. *Int. J. Heat Fluid Flow* **1992**, *13*, 294–299.
- (20) Spirkl, W.; Ries, H. Optimal finite-time endoreversible processes. *Phys. Rev. E* **1995**, *52*, 3485.
- (21) Johannessen, E.; Røsjorde, A. Equipartition of entropy production as an approximation to the state of minimum entropy production in diabatic distillation. *Energy* **2007**, *32*, 467–473.
- (22) Andresen, B. Current Trends in Finite-Time Thermodynamics. *Angew. Chem., Int. Ed.* **2011**, *50*, 2690–2704.

- (23) Curzon, F.; Ahlborn, B. Efficiency of a Carnot engine at maximum power output. *Am. J. Phys.* **1975**, *43*, 22–24.
- (24) Rubin, M. H. Optimal configuration of a class of irreversible heat engines. I. *Phys. Rev. A* **1979**, *19*, 1272.
- (25) Salamon, P.; Nitzan, A. Finite time optimizations of a Newton’s law Carnot cycle. *J. Chem. Phys.* **1981**, *74*, 3546–3560.
- (26) Salamon, P.; Andresen, B.; Gait, P. D.; Berry, R. S. The significance of Weinhold’s length. *J. Chem. Phys.* **1980**, *73*, 1001–1002.
- (27) Weinhold, F. Metric geometry of equilibrium thermodynamics. *J. Chem. Phys.* **1975**, *63*, 2479–2483.
- (28) Salamon, P.; Berry, R. S. Thermodynamic length and dissipated availability. *Phys. Rev. Lett.* **1983**, *51*, 1127–1130.
- (29) Badescu, V. *Modelling Thermodynamic Distance, Curvature and Fluctuations: A Geometric Approach*; Springer International Publishing AG: Cham, Switzerland, 2008.
- (30) Onsager, L. Reciprocal Relations in Irreversible Processes. I. *Phys. Rev.* **1931**, *37*, 405–426.
- (31) Onsager, L. Reciprocal Relations in Irreversible Processes. II. *Phys. Rev.* **1931**, *38*, 2265–2279.
- (32) Diosi, L.; Kulacsy, K.; Lukacs, B.; Racz, A. Thermodynamic length, time, speed, and optimum path to minimize entropy production. *J. Chem. Phys.* **1996**, *105*, 11220–11225.
- (33) Salamon, P.; Nulton, J.; Siragusa, G.; Limon, A.; Bedeaux, D.; Kjelstrup, S. A simple example of control to minimize entropy production. *J. Non-Equilib. Thermodyn.* **2002**, *27*, 45–55.

- (34) Schaller, M.; Hoffmann, K. H.; Siragusa, G.; Salamon, P.; Andresen, B. Numerically optimized performance of diabatic distillation columns. *Comput. Chem. Eng.* **2001**, *25*, 1537–1548.
- (35) de Koeijer, G. M.; Kjelstrup, S.; Salamon, P.; Siragusa, G.; Schaller, M.; Hoffmann, K. H. Comparison of entropy production rate minimization methods for binary diabatic distillation. *Ind. Eng. Chem. Res.* **2002**, *41*, 5826–5834.
- (36) Ruppeiner, G. Implementation of an adaptive, constant thermodynamic speed simulated annealing schedule. *Nucl. Phys. B, Proc. Suppl.* **1988**, *5*, 116–121.
- (37) Hoffmann, K. H.; Salamon, P. The optimal simulated annealing schedule for a simple model. *J. Phys. A: Math. Gen.* **1990**, *23*, 3511.
- (38) Andresen, B.; Gordon, J. M. Constant thermodynamic speed for minimizing entropy production in thermodynamic processes and simulated annealing. *Phys. Rev. E* **1994**, *50*, 4346–4351.
- (39) Magnanelli, E.; Wilhelmsen, Ø.; Johannessen, E.; Kjelstrup, S. Minimum entropy production in optimally controlled membrane processes. *In progress*
- (40) Kjelstrup, S.; Bedeaux, D. *Non-equilibrium thermodynamics of heterogeneous systems*; World Scientific: Singapore, 2008; Vol. 16.
- (41) Berry, R. S. *Thermodynamic optimization of finite-time processes*; J. Wiley: Hoboken, New Jersey, 2000.
- (42) Nulton, J.; Salamon, P.; Andresen, B.; Anmin, Q. Quasistatic processes as step equilibrations. *J. Chem. Phys.* **1985**, *83*, 334–338.
- (43) Baker, R. W. Future directions of membrane gas separation technology. *Ind. Eng. Chem. Res.* **2002**, *41*, 1393–1411.

- (44) Magnanelli, E.; Wilhelmsen, Ø.; Johannessen, E.; Kjelstrup, S. Enhancing the understanding of heat and mass transport through a cellulose acetate membrane for CO<sub>2</sub> separation. *J. Mem. Sci.* **2016**, *513*, 129–139.
- (45) Houde, A.; Krishnakumar, B.; Charati, S.; Stern, S. Permeability of dense (homogeneous) cellulose acetate membranes to methane, carbon dioxide, and their mixtures at elevated pressures. *J. Appl. Polym. Sci.* **1996**, *62*, 2181–2192.
- (46) Nummedal, L.; Røsjorde, A.; Johannessen, E.; Kjelstrup, S. Second law optimization of a tubular steam reformer. *Chem. Eng. Process.* **2005**, *44*, 429–440.

# TOC-graphic

